HIBISCUS PUBLISHER

JOURNAL OF ENVIRONMENTAL MICROBIOLOGY AND TOXICOLOGY

Website: https://journal.hibiscuspublisher.com/index.php/JEMAT

Modelling the Inhibitory Effect of SiO_2-coated Zero-valent Iron/palladium Bimetallic Nanoparticles (Sio_2-nZVI/Pd) Reductant on *Pseudomonas putida* as the Biocatalyst for 2,2',4,4'-tetrabromodiphenyl ether Degradation

Bilal Ibrahim Dan-Iya,[1,2]* Ibrahim Alhaji Sabo[3] and Salihu Yahuza[4]

[1]Department of Biomedical Sciences and Biotechnology, School of Health Sciences, International Medical University, Bukit Jalil, 57000 Kuala Lumpur, Malaysia.
[2]Pharmacy Technician Department, College of Health Sciences and Technology, Kano Nigeria.
[3]Department of Microbiology, Faculty of Pure and Applied Sciences, Federal University Wukari, P.M.B. 1020 Wukari, Taraba State Nigeria.
[4]Department of Microbiology and Biotechnology, Federal University Dutse, PMB 7156, Dutse, Jigawa State, Nigeria.

*Corresponding author:

Bilal Ibrahim Dan-Iya
Pharmacy Technician Department,
College of Health Sciences and Technology,
Kano Nigeria.
Email: bidaniya@gmail.com

HISTORY

Received: 25th Feb 2020
Received in revised form: 14th of March 2020
Accepted: 18th of May 2020

KEYWORDS

SiO2-coated Bimetallic Nanoparticles
P. putida
Growth
Mathematical model
Buchanan-3-phase

ABSTRACT

The used of linearization technique using natural logarithm transformation, though standard, is erroneous and can just give an estimated value for the sole parameter measured; the specific growth rate. in this paper, for the first time we model the effect of nZVI/Pd and SiO_2-nZVI/Pd nanoparticles on the growth of *P. putida* in MSM medium as modelled using models such as von Bertalanffy, Baranyi-Roberts, modified Schnute, modified Richards, modified Gompertz, modified logistics and the most recent Huang. The results show that the lag phases of *P. putida* cell at 4 h (0.5 g L^{-1} of SiO_2-nZVI/Pd), 7.655 h (1.0 g L^{-1} of SiO_2-nZVI/Pd), 11.76 h (0.5 g L^{-1} of nZVI/Pd) and 22.03 h (1.0 g L^{-1} of nZVI/Pd) respectively, which were longer than that of control, indicating the nanoparticles prolonged the exponential phase of cell growth. Moreover, in comparing the maximum growth $y_{max,}$ which was $1.23x10^9$, there was a decrease in the *P. putida* growth, i.e $1.20x10^9$ (0.5 g L^{-1} of SiO_2-nZVI/Pd), $1.06x10^9$ (1.0 g L^{-1} of SiO_2-nZVI/Pd), $1.04x10^9$ (0.5 g L^{-1} of nZVI/Pd) and $8.59x10^8$ (1.0 g L^{-1} of nZVI/Pd) respectively, with more decrease in growth at the *P. putida* growth with nZVI/Pd than SiO_2-nZVI/Pd. On the other hand, when comparing the $\mu_{max,}$ the control has a value of 0.08 while 0.073, 0.073, 0.089 and 0.86 are values at bacterial concentration of (0.5 g L^{-1} of SiO_2-nZVI/Pd), (1.0 g L^{-1} of SiO_2-nZVI/Pd), (0.5 g L^{-1} of nZVI/Pd) and (1.0 g L^{-1} of nZVI/Pd) respectively, indicating the specific growth rate decreases with both 0.5 g L^{-1} of SiO_2-nZVI/Pd and 1.0 g L^{-1} of SiO_2-nZVI/Pd and increases with 0.5 g L^{-1} of nZVI/Pd and 1.0 g L^{-1} of nZVI/Pd. It is clear from the results that coating of SiO_2 on nZVI/Pd might drastically decrease the toxicity to *P. putida* cells.

INTRODUCTION

Mathematical modeling has proved to be an effective method for researching viral pathogenesis and has provided understanding into the dynamics of intracellular viral and bacterial infections, the role of the immune system, the assessment of strategies involving treatment and the occurrence of resistance to drug [1]. Modeling may expand our knowledge on various scales: from the intracellular pathogen-host molecular scale interactions, to population-scale extracellular cell to cell invasion, to pathogen dissemination inside organs or entire species [1]. To quantitatively research at molecular level bacterial or viral growth and to examine host needs and constraints, Bacteriophages intracellular models, Baculovirus and Semliki forest virus have been firstly established. the human immunodeficiency virus offered understanding into the pathogenesis, strategies of treatment and virus monitoring by studying it's cell to cell infection [1]. Mechanical mathematical

models can be a crucial instrument in shaping our insight of multiplex biological systems. In recent years, various mathematical models of interaction amongst pathogens and immune responses of host have been established, with bacterial pathogens researched including *mycobacterium Tuber-culosis*, *Bacillus anthracis* and *Streptococcus pneumoniae* [2].

Normally, bacterial growth curve shows sigmoidal pattern, beginning with lag phase after t=0, then the logarithmic phase and then bacteria moves into the stationary section and finally enters the death section or bacterial growth declining phase. Different sigmoidal functions were used to describe bacterial growth curve, these sigmoidal functions include modified Gompertz, Modified logistics and Stannard, Von Bertalanffy, Baranyi-Roberts, Stannard, von Bertalanffy, Baranyi-Roberts, modified Schnute and Modified Richards [3]. Comprehensive statistical model that comprises of rest of other models was used to compare them (Schnute model). In the F test that was used, unfitness of the models was assessed (compared) with the measuring error while with the t test that was also used, intervals of confidence for issues can be projected and be used to differentiate models. Additionally, comparison between models was done by considering the flexibility of utilization. in a quest to comprise all relevant biological issues, sigmoidal functions were all amended. Richards, Stannard and Schnute models appeared to be fundamentally the same equation [4,5]. Viewing the tested cases, the growth data of caffeine was statistically explained by the Modified Gompertz equation. The important growth curve issues are the lag time, maximum specific growth rate (μ_{max}) and asymptotic value. During secondary models, maximum specific growth rate (μ_{max}) may be used to investigate the impacts of product on growth rate, substrate, pH and temperature.

Empirical and mechanistic properties are features that most bacterial growth models lie between them, however, the possibility of these two categories to occur in reality side by side is anticipated [6]. In this work, we present for the first time the use of primary models in modelling the *Caulobacter crescentus* growth curve. As the advantages of nonlinear regression analysis on bacterial growth have been described above, thus, the objective of this finding is to assess several available models such as Buchanan three-phase [4], Gompertz [3,7], schnute [3], Logistic [3,8], Von Bertalanffy [9,10], Richards [3,11], Baranyi-roberts [5] and more recently the Huang model [6]. In this study, we show for the first time the applicability of the Huang model in modelling the inhibitory effect of SiO_2-coated zero-valent iron/palladium bimetallic nanoparticles (SiO_2-nZVI/Pd) reductant on *Pseudomonas putida* as the biocatalyst for 2,2',4,4'-tetrabromodiphenyl ether degradation.

MATERIALS AND METHODS

Data from fig 2a. from [12]) was processed using the software Webplotdigitizer 2.5 [13] which digitizes the scanned figure and has been utilized by many researchers and acknowledged for its reliability [14,15].

Statistical Analysis

Statistical significant difference between the models was calculated through various methods including the adjusted coefficient of determination (R^2), accuracy factor (AF), bias factor (BF), root-mean-square error (RMSE) and corrected AICc (Akaike information criterion) as before [14].

Fitting of the Data

Fitting of the bacterial growth curve using various growth models (**Table 1**) was carried out using the Curve expert professional software (version 1.6) by nonlinear regression using the Marquardt algorithm. Modelling is done after converting data to logarithmic values. The μ_{max} of estimation was carried out by the steepest ascent rifle of the curve while the crossing of this line with the x-axis is an estimation of λ. The highest growth was chosen for the modelling exercise.

Table 1. Growth models used in this study.

model	p	Equation
Modified Logistic	3	$y=\frac{A}{\left\{1+\exp\left[\frac{4\mu_m}{A}(\lambda-t)+2\right]\right\}}$
Modified Gompertz	3	$y=A\exp\left\{-\exp\left[\frac{\mu_m e}{A}(\lambda-t)+1\right]\right\}$
Modified Richards	4	$y=A\left\{1+v\exp(1+v)\exp\left[\frac{\mu_m}{A}(1+v)\left(1+\frac{1}{v}\right)(\lambda-t)\right]\right\}^{\left(\frac{-1}{v}\right)}$
Modified Schnute	4	$y=\left(\mu_m\frac{(1-\beta)}{\alpha}\right)\left[\frac{1-\beta\exp(\alpha\lambda+1-\beta-\alpha t)}{1-\beta}\right]^{\frac{1}{\beta}}$
Baranyi-Roberts	4	$y=A+\mu_m x+\frac{1}{\mu_m}\ln\left(e^{-\mu_m x}+e^{-h_0}-e^{-\mu_m x-h_0}\right)-\ln\left(1+\frac{e^{\mu_m x+\frac{1}{\mu_m}\ln\left(e^{-\mu_m x}+e^{-h_0}-e^{-\mu_m x-h_0}\right)}-1}{e^{(y_{max}-A)}}\right)$
Von Bertalanffy	3	$y=K\left[1-\left[1-\left(\frac{A}{K}\right)^3\right]\exp^{-\left(\mu_m x/3K^{\frac{1}{3}}\right)}\right]^3$
Huang	4	$y=A+y_{\max}-\ln\left(e^A+\left(e^{Y\max}-e^A\right)e^{-\mu_m B(x)}\right)$ $B(x)=x+\frac{1}{\alpha}\ln\frac{1+e^{-\alpha(x-\lambda)}}{1+e^{\alpha\lambda}}$
Buchanan Three-phase linear model	3	y = A, if x < lag y=A + k(x−λ), if λ ≤ x ≥x_{max} y = y_{max}, if x ≥ x_{max}

Note:
A= *P. putida* growth lower asymptote;
y_{max}= *P. putida* growth upper asymptote;
μ_{max}= maximum specific *P. putida* growth rate;
v= affects near which asymptote maximum growth occurs.
λ=lag time
e = exponent (2.718281828)
t = sampling time
A,B, k = curve fitting parameters
h_0 = a dimensionless parameter quantifying the initial physiological state of the reduction process. the lag time (h^{-1}) or (d^{-1}) can be calculated as h_0= μ_{max}

RESULTS AND DISCUSSION

All of the curves tested show visually acceptable fitting (**Figs 2 to 8)**. Growth data should be converted to log unit before modelling is carried out. The best performance was the Huang model with the lowest value for RMSE, AICc and the highest value for adjusted R^2. the AF and BF values were also excellent for the model with their values were the closest to 1.0. The poorest performance was the Modified Richard model (**Table 2**). the coefficients for the Huang model are shown in **Table 3**.

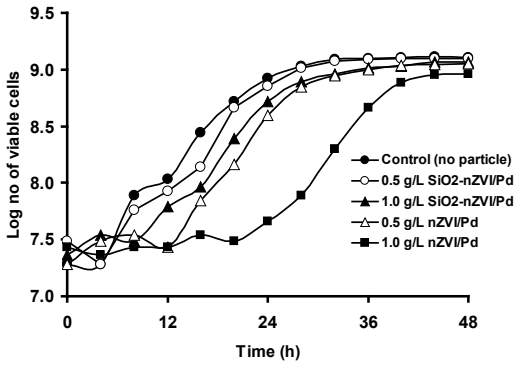

Fig 1. Replotted data on the effect of nZVI/Pd and SiO_2-nZVI/Pd nanoparticles on the log growth of *P. putida* in MSM medium.

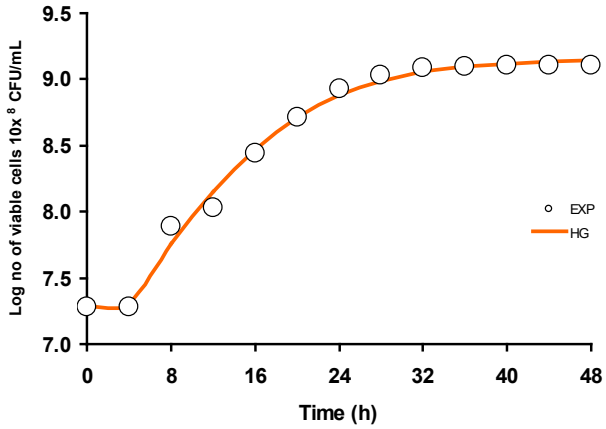

Fig. 2. The effect of nZVI/Pd and SiO_2-nZVI/Pd nanoparticles on the growth of *P. putida* in MSM medium as modelled using the Huang model.

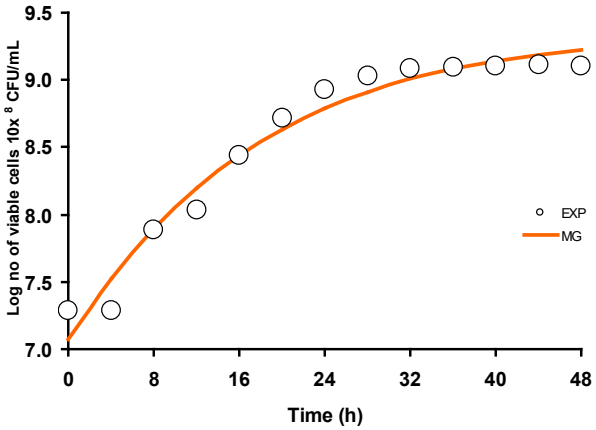

Fig. 3. The effect of nZVI/Pd and SiO_2-nZVI/Pd nanoparticles on the growth of *P. putida* in MSM medium as modelled using the modified Gompertz model.

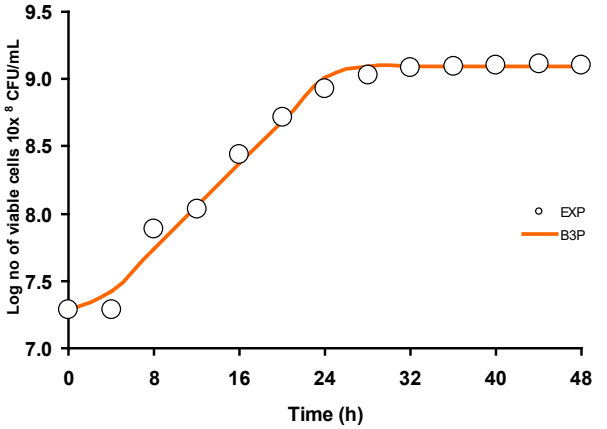

Fig. 4. The effect of nZVI/Pd and SiO_2-nZVI/Pd nanoparticles on the growth of *P. putida* in MSM medium as modelled using the buchanan-3-phase model.

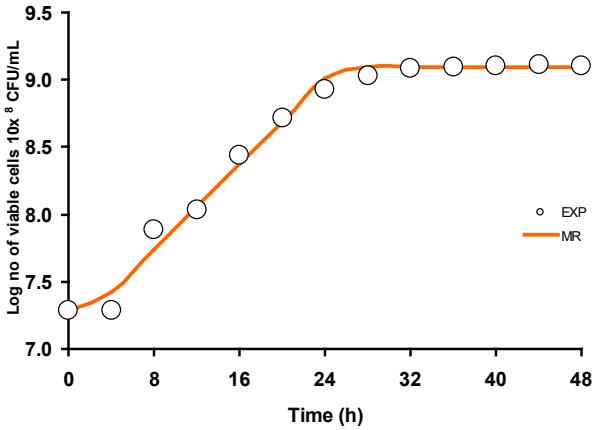

Fig. 5. The effect of nZVI/Pd and SiO_2-nZVI/Pd nanoparticles on the growth of *P. putida* in MSM medium as modelled using the modified Richard model.

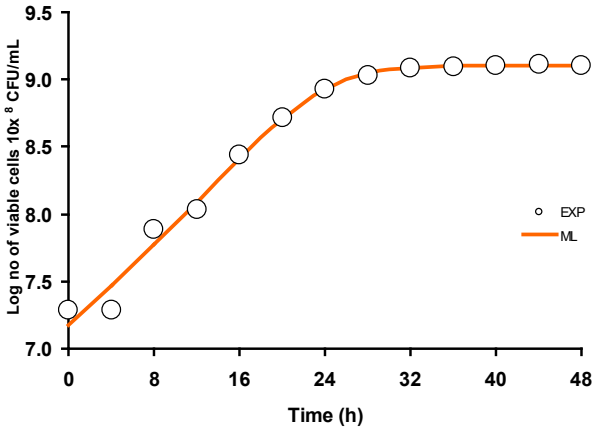

Fig. 6. The effect of nZVI/Pd and SiO_2-nZVI/Pd nanoparticles on the growth of *P. putida* in MSM medium as modelled using the modified logistics model.

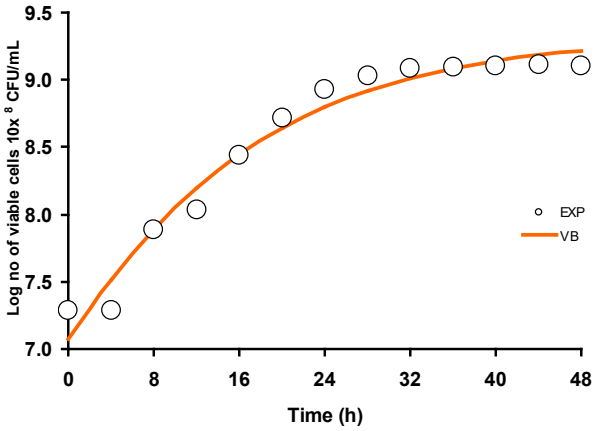

Fig. 7. The effect of nZVI/Pd and SiO_2-nZVI/Pd nanoparticles on the growth of *P. putida* in MSM medium as modelled using the von Bertalanffy model.

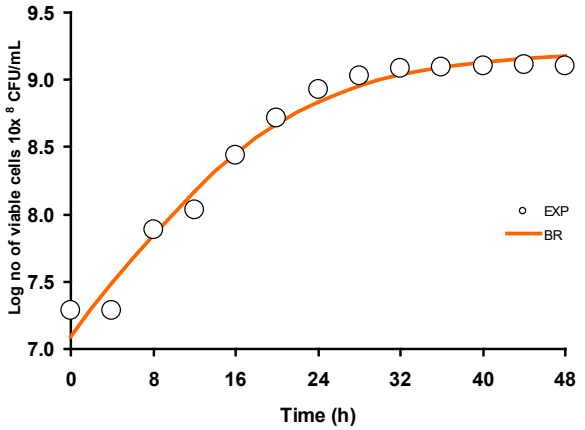

Fig. 8. The effect of nZVI/Pd and SiO_2-nZVI/Pd nanoparticles on the growth of *P. putida* in MSM medium as modelled using the Baranyi-Roberts model.

Table 2. Statistical tests for the various models utilized in modelling the effect of nZVI/Pd and SiO_2-nZVI/Pd nanoparticles on the growth of *P. putida* in MSM medium.

Model	*P* RMSE	R^2	adR^2	AF	BF	AICc
Huang	4 0.07	0.99	0.99	1.00	1.00	-48.98
Baranyi-Roberts	4 0.12	0.98	0.97	1.01	1.00	-33.88
Modified Gompertz	3 0.14	0.97	0.95	1.01	1.00	-35.45
Buchanan-3 phase	3 0.08	0.99	0.99	1.01	1.00	-51.32
Modified Richards	4 0.08	0.99	0.98	1.01	1.00	-42.61
Modified Schnute	3 0.11	0.98	0.97	1.01	1.00	-35.10
Modified Logistics	3 0.14	0.97	0.96	1.01	1.00	-36.42
Von Bertalanffy	4 0.34	0.75	0.67	1.03	1.00	-12.78

Note: p is no. of parameter

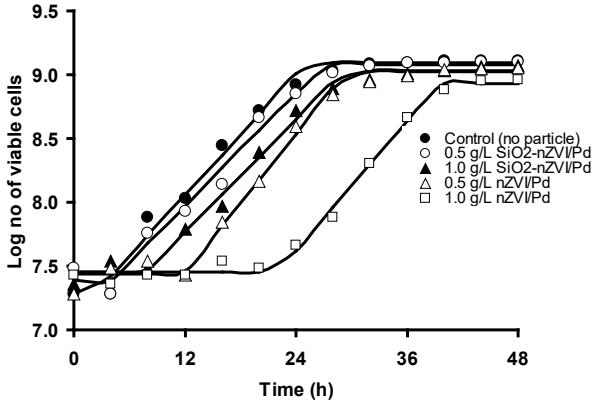

Fig 9. Modelling of the log growth of *P. putida* on various diets using the Buchanan-3-phase model.

The choice of the Buchanan as the best model is apt since the model is the simplest amongst the eight and it is a three-parameter model giving it a higher degree of freedom compared to four- or five-parameter models. This is important when a growth curve having a smaller number of points is used. In addition, all three parameters have biological meaning due to the highly mechanistic property of the model. The Buchanan three-phase model has been successfully used to model growth of bacteria (Abou-zeid *et al.,* 2007; Baranyi, 1998; Caleb, Mahajan, Al-said, & Opara, 2013; Singh & Srivastava, 2014), algae [16] and worm [17].

Nonlinear regression of the Baranyi-Roberts model could be problematic in some cases as it is rather sensitive to the number and distribution of data points (Buchanan *et al.*, 1997; Baranyi, 1997). Buchanan *et al.* (1997) developed a simpler three-phase linear model to overcome this problem,
The assumptions of the Buchanan model were as follows;
(i) That the specific growth rate is equal to zero during the lag phase,
(ii) The logarithm of the bacterial cells increases linearly with respect to time during the exponential phase and
(iii) The specific growth rate is zero during the stationary phase.

These assumptions can be expressed as follows;
lag phase:
for $t \leq t_{lag}$,
$n_t = n_o$
Exponential growth phase:
for $t_{lag} < t < t_{max}$,
$n_t = n_o + \mu (t - t_{lag})$
Stationary phase:
for $t \geq t_{max}$,
$n_t = n_{max}$

Where n_o = log of initial population density (optical density) or bacterial cell number (CFU/ml); n_t = log population density (optical density) or bacterial cell number (CFU/ml) at time t; n_{max} = log of the maximal population density (optical density) or bacterial cell number (CFU/ml); t = elapsed time (h); t_{max} = time (h) when the maximum population density (optical density) or bacterial cell number (CFU/ml) is reached; t_{lag} = time (h) at the end of the lag phase and μ = specific growth rate (log (CFU/ml)/h).

The Buchanan model greatest advantage is its straightforwardness. additionally, it supplies an approximation to the mathematical means microbiologists have usually used to calculate growth kinetic graphically (Buchanan et al., 1997). Its disadvantage include the fact that it could only fit growth curves having an abrupt transition from the lag phase to exponential phase [18].

It has been suggested that when a three-parameter model is sufficient to describe the data, experts recommend over a four-parameter model given that the three-parameter model is much simpler and as a consequence much easier to use and solution is more stable considering that the parameters are much less correlated. On top of that, every time a three-parameter model is employed, the estimates have more degrees of freedom, and this can be crucial every time a growth curve or generation curve with a small number of measured points is employed. In addition, it is essential that all three parameters may be given a biological interpretation.

Table 3. Growth coefficients as modelled using the Huang model.

Param-eters	Control (no particle)		0.5 g/L SiO_2-nZVI/Pd		1.0 g/L SiO_2-nZVI/Pd		0.5 g/L nZVI/Pd		1.0 g/L nZVI/Pd	
	Value	95% CI	Value	95% CI	Value	95% CI	Value	95% CI	Value	95% CI
lag (h)	2.26	-0.72 to 5.24	4	0.794 to 7.206	7.655	5.52 to 9.789	11.76	9.885 to 13.64	22.03	20.34 to 23.71
y_{max}	$1.23x10^9$	$1.04x10^9$ to $1.46x10^9$	$1.20x10^9$	$1.00x10^9$ to $1.43x10^9$	$1.06x10^9$	$9.10x10^8$ to $1.24x10^9$	$1.04x10^9$	$9.0x10^8$ to $1.24x10^9$	$8.59x10^8$	$7.23x10^8$ to $1.02x10^9$
μ_{max}	0.08	0.069 to 0.091	0.073	0.059 to 0.088	0.073	0.064 to 0.082	0.089	0.076 to 0.103	0.086	0.071 to 0.1

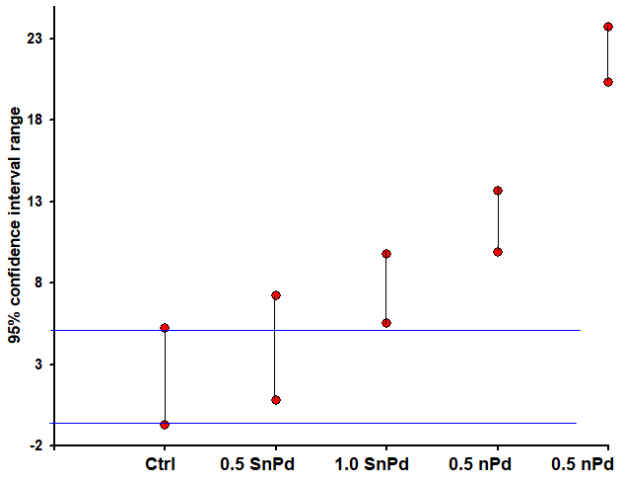

Fig. 10. Shukor's Confidence interval chart for lag period of *P. putida* growth as modelled to the Buchanan-3-phase model in assessing significant difference between treatment of various nanoparticles (0.5 g/L SiO_2-nZVI/Pd (0.5 SnPd), 1.0 g/L SiO_2-nZVI/Pd (1.0 SnPd), 0.5 g/L nZVI/Pd (0.5 nPd) and 1.0 g/L nZVI/Pd (1.0 nPd)) in comparison to control.

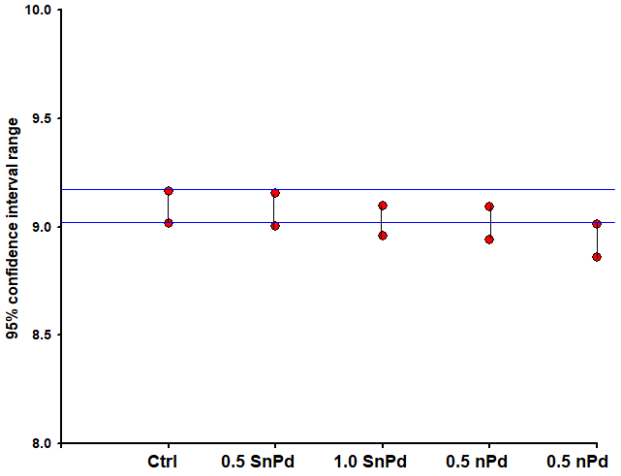

Fig. 11. Shukor's confidence interval chart for y_{max} of *P. putida* growth as modelled to the Buchanan-3-phase model in assessing significant difference between treatment of various nanoparticles (0.5 g/L SiO_2-nZVI/Pd (0.5 SnPd), 1.0 g/L SiO_2-nZVI/Pd (1.0 SnPd), 0.5 g/L nZVI/Pd (0.5 nPd) and 1.0 g/L nZVI/Pd (1.0 nPd)) in comparison to control.

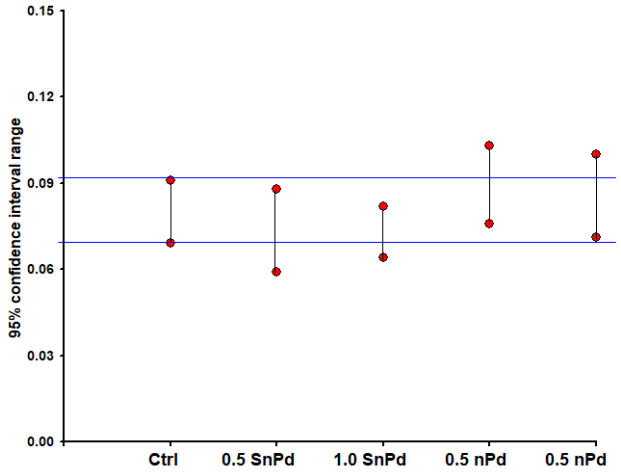

Fig. 12. Shukor's confidence interval chart for M_{max} of *P. putida* growth as modelled to the Buchanan-3-phase model in assessing significant difference between treatment of various nanoparticles (0.5 g/l SiO_2-nZVI/Pd (0.5 SnPd), 1.0 g/l SiO_2-nZVI/Pd (1.0 SnPd), 0.5 g/l nZVI/Pd (0.5 nPd) and 1.0 g/l nZVI/Pd (1.0 nPd)) in comparison to control.

In general, for nonlinear regression, overlapping of the 95% confidence intervals indicate no significant differences while nonoverlap confidence interval indicates the opposite [19,20]. Compared with control which was 2.26 h, lag phases of *P. putida* cell were 4 h (0.5 g L^{-1} of SiO_2-nZVI/Pd), 7.655 h (1.0 g L^{-1} of SiO_2-nZVI/Pd), 11.76 h (0.5 g L^{-1} of nZVI/Pd) and 22.03 h (1.0 g L^{-1} of nZVI/Pd) respectively, which were longer than that of control, indicating the nanoparticles prolonged the exponential phase of cell growth. Moreover, in comparing the maximum growth y_{max}, which was $1.23x10^9$, there is decrease in the *P. putida* growth, i.e $1.20x10^9$ (0.5 g L^{-1} of SiO_2-nZVI/Pd), $1.06x10^9$ (1.0 g L^{-1} of SiO_2-nZVI/Pd), $1.04x10^9$ (0.5 g L^{-1} of nZVI/Pd) and $8.59x10^8$ (1.0 g L^{-1} of nZVI/Pd) respectively, with more decrease in growth at the *P. putida* growth with nZVI/Pd than SiO_2-nZVI/Pd. On the other hand, when comparing the μ_{max}, the control has a value of 0.08 while 0.073, 0.073, 0.089 and 0.86 are values at bacterial concentration of (0.5 g L^{-1} of SiO_2-nZVI/Pd), (1.0 g L^{-1} of SiO_2-nZVI/Pd), (0.5 g L^{-1} of nZVI/Pd) and (1.0 g L^{-1} of nZVI/Pd) respectively, indicating the specific growth rate decreases with both 0.5 g L^{-1} of SiO_2-nZVI/Pd and 1.0 g L^{-1} of SiO_2-nZVI/Pd and increases with 0.5 g L^{-1} of

nZVI/Pd and 1.0 g L^{-1} of nZVI/Pd. It is clear from the results that coating of SiO_2 on nZVI/Pd might drastically decrease the toxicity to *P. putida* cells.

Parameters obtained from the fitting exercise were maximum growth rate (μ_{max}), lag time (λ) and maximal growth (y_{max}). The three biologically meaningful coefficients can be later used for secondary modelling using model such as the two-parameter Monod model or other more complex models "secondary models" such as Haldane, Aiba, Yano and others. These mechanistic models are used in basic research and are aimed to reach a better understanding of the physical, chemical and biological processes that lead to the growth profile seen. All other things being equal, mechanistic models are more powerful since they tell you about the underlying processes driving patterns. They are more likely to work correctly when extrapolating beyond the observed conditions [21].

CONCLUSION

In conclusion, the Buchanan-3-phase model was the best model based on statistical tests such as corrected AICc (Akaike information criterion), bias factor (BF), adjusted coefficient of determination (R^2) and root-mean-square error (RMSE). The results show that the lag phases of *P. putida* cells were longer than that of control, indicating the nanoparticles prolonged the exponential phase of cell growth. Moreover, in comparing the maximum growth $y_{max,}$ a decrease in growth of *P. putida* occurs more with nZVI/Pd than SiO_2-nZVI/Pd. On the other hand, when comparing the $\mu_{max,}$ the specific growth rate decreases with both 0.5 g L^{-1} of SiO_2-nZVI/Pd and 1.0 g L^{-1} of SiO_2-nZVI/Pd and increases with 0.5 g L^{-1} of nZVI/Pd and 1.0 g L^{-1} of nZVI/Pd. It is clear from the results that coating of SiO_2 on nZVI/Pd might drastically decrease the toxicity to *P. putida* cells. The use of bacterial growth models to obtained exact growth rate is advantageous for further development of secondary model and this work has revealed the capability of such models.

ACKNOWLEDGEMENT

The authors wish to acknowledge the hard work of their academic mentor, Professor Dr. Mohd Yunus Abd Shukor and Petroleum Technology Development Fund (PTDF) and the Tertiary Education Trust Fund (TETFund) for funding their researches.

REFERENCES

1. Zitzmann C, Kaderali L. Mathematical analysis of viral replication dynamics and antiviral treatment strategies: From basic models to age-based multi-scale modeling. Front Microbiol. 2018;9(JUL):1–18.
2. Best A, Jubrail J, Boots M, Dockrell D, Marriott H. A mathematical model shows macrophages delay Staphylococcus aureus replication, but limitations in microbicidal capacity restrict bacterial clearance. J Theor Biol. 2020;497.
3. Zwietering MH, Jongenburger I, Rombouts FM, Van't Riet K. Modeling of the bacterial growth curve. Appl Environ Microbiol. 1990;56(6):1875–81.
4. Buchanan RL. Predictive food microbiology. Trends Food Sci Technol. 1993;4(1):6–11.
5. Baranyi J. Mathematics of predictive food microbiology. Int J Food Microbiol. 1995;26(2):199–218.
6. Huang L. Optimization of a new mathematical model for bacterial growth. Food Control. 2013;32(1):283–8.
7. Gompertz B. On the nature of the function expressiveness of the law of human mortality, and a new mode of determining the value of life contingencies. Philos TransR Soc Lond. 1825;115:513 – 585.
8. Ricker WE. 11 Growth Rates and Models. 1979. 677 p. (Fish Physiology; vol. 8).
9. Babák L, Šupinová P, Burdychová R. Growth models of Thermus aquaticus and Thermus scotoductus. Acta Univ Agric Silvic Mendel Brun. 2012;60(5):19–26.
10. López S, Prieto M, Dijkstra J, Dhanoa MS, France J. Statistical evaluation of mathematical models for microbial growth. Int J Food Microbiol. 2004;96(3):289–300.
11. Richards FJ. A flexible growth function for empirical use. J Exp Bot. 1959;10:290–300.
12. Lv Y, Niu Z, Chen Y, Hu Y. Synthesis of SiO2 coated zero-valent iron/palladium bimetallic nanoparticles and their application in a nano-biological combined system for 2,2′,4,4′-tetrabromodiphenyl ether degradation. RSC Adv. 2016 Feb 16;6(24):20357–65.
13. Rohatgi A. WebPlotDigitizer. http://arohatgi.info/WebPlotDigitizer/app/ Accessed June 2 2014.; 2015.
14. Halmi MIE, Shukor MS, Johari WLW, Shukor MY. Modeling the growth curves of *Acinetobacter* sp. strain DRY12 grown on diesel. J Environ Bioremediation Toxicol. 2014;2(1):33–7.
15. Khare KS, Phelan Jr FR. Quantitative comparison of atomistic simulations with experiment for a cross-linked epoxy: A specific volume–cooling rate analysis. Macromolecules. 2018;51(2):564–575.
16. Collins S. Competition limits adaptation and productivity in a photosynthetic alga at elevated CO2. Proc R Soc B Biol Sci. 2011;278(1703):247–55.
17. Nieminen JK. Enchytraeid population dynamics: Resource limitation and size-dependent mortality. Ecol Model. 2009;220(11):1425–30.
18. Li H, Xie G, Edmondson A. Evolution and limitations of primary mathematical models in predictive microbiology. Br Food J. 2007;109(8):608–26.
19. Wijtzes T, Wit, Veld JHJ, Riet, t van, Zwietering M. Modelling bacterial growth of *Lactobacillus curvatus* as a function of acidity and temperature. Appl Environ Microbiol 61 1995 2533-2539. 1995 Jan 1;61.
20. Schenker N, Gentleman JF. On judging the significance of differences by examining the overlap between confidence intervals. Am Stat. 2001;55(3):182–6.
21. Bolker BM. Ecological Models and Data in R. Princeton, N.J: Princeton University Press; 2008. 408 p.